Biochimica et Biophysica Acta, 692 (1982) 1–17
Elsevier Biomedical Press

BBA 71300

ON THE MICROSTRUCTURE AND PHASE DIAGRAM OF DIMYRISTOYLPHOSPHATIDYLCHOLINE-GLYCOPHORIN BILAYERS

THE ROLE OF DEFECTS AND THE HYDROPHILIC LIPID-PROTEIN INTERACTION *

D. RÜPPEL, H.-G. KAPITZA, H.J. GALLA, F. SIXL and E. SACKMANN

Abteilung für Biophysik, Universität Ulm, D-7900 Ulm and Physik Department E22, Technische Universität München, D-8046 Garching bei München (F.R.G.)

(Received April 20th, 1982)

Key words: Glycophorin; Dimyristoylphosphatidylcholine; Lipid-protein interaction; Conformational change; Defect; Phase diagram

Glycophorin-dimyristoylphosphatidylcholine bilayers were studied at the limit of low protein concentrations by a number of different techniques. These included freeze-fracture electron microscopy, calorimetry, electron paramagnetic resonance spectroscopy, the photobleaching technique and energy transfer measurements. The liquidus and solidus lines of the dimyristoylphosphatidylcholine-glycophorin system were determined by differential thermal analysis. Structural information was obtained from changes in the texture of the freeze-fracture micrographs. Electron microscopy, together with diffusion measurements, established the important role of linear defects in the solid lipid phases for the incorporation of small amounts of glycophorin and for the fast transport of the protein. Particles were observed above 1 mol‰ of protein content, below 10°C, which form due to the immiscibility of glycophorin in the crystalline lipid phase. Lipid-protein aggregates are expelled from the bilayer into the aqueous phase. The concentration dependence of the energy transfer between fluorescein- and eosin-carrying protein headgroups is interpreted in terms of a two-conformation model: At low concentrations ($x_p < 0.8$ mol‰) the carbohydrate-carrying headgroup spreads at the lipid-water interface forming a two-dimensional (pancake-like) structure, while at higher concentrations the headgroup starts to assume a three-dimensional conformation protruding into the aqueous phase. The concentration dependence of the heat of transition led to the conclusion that one protein molecule interacts with about 300 lipid molecules in the first conformation and with about 100 lipids in the second one. The high number of protein-bound lipids is explained by hydrophilic lipid-protein interaction. All experiments demonstrated that the protein concentration of 0.8 mol‰ plays a critical role. (1) The solidus line starts to exhibit a horizontal deflection between 0.4 and 3.2 mol‰ demonstrating solid state phase separation. (2) The spin label order parameter in the fluid lipid phase exhibits a minimum, indicating a maximum in the lipid packing density. (3) The regular ripple phase completely vanishes at 0.4 ‰ while it reappears at higher concentrations. This is related to a headgroup conformational change. The results are summarized in a tentative phase diagram of the dimyristoylphosphatidylcholine-glycophorin system.

Introduction

Glycophorin, an integral protein of the erythrocyte membrane, is a bipolar amphiphatic macromolecule consisting of three parts [1]: (1) a

* Dedicated to Professor A. Weller at the occasion of his 60th birthday.

0005-2736/82/0000–0000/$02.75

hydrophobic α-helical core of 32 amino acids (M_r 3300), (2) a hydrophilic carboxylic end of 35 amino acids (M_r 3900) and (3) an NH_2-terminal segment of 64 amino acids to which 16 oligosaccharides are linked (M_r 25900).

One saccharide chain has 11 or 13 monomers [2,3], the others 5 or 6 [4]. They are usually terminated by sialic acids. These contribute up to 32 negative charges to the headgroup. Since the glycosylated headgroup is large compared to the hydrophobic core, glycophorin also possesses the features of a peripheral protein. Due to its structural ability to incorporate into lipid bilayers [5] it is very well suited for model membrane studies.

The present work reports on the interaction of glycophorin with dimyristoylphosphatidylcholine in lipid bilayer membranes. In contrast to most previous studies [5–8] our attention was mainly directed to very low protein concentrations (0.2–4 ‰). The results obtained by freeze-fracture electron microscopy, calorimetry, photobleaching technique, spin label paramagnetic resonance and measurements of intermolecular energy transfer between dyes linked to either proteins or lipids are compared.

Materials and Methods

Lipids, protein isolation and membrane reconstitution

Dimyristoylphosphatidylcholine (DMPC) was a commercial product of Fluka. Glycophorin A was prepared from human erythrocytes. Ghosts were obtained according to Dodge et al. [9] by hemolysis in a phosphate buffer (5 mM). The freeze-dried ghosts were dissolved in a sodium deoxycholate solution (25 mM Tris-HCl buffer of pH 7.4, 10 mM deoxycholate). This solution was dialyzed extensively against distilled water and contained a residual deoxycholate concentration of 1 mol per mol glycophorin A [10].

The crude protein was purified chromatographically on a wheat germ lectin-sepharose column (Sepharose 6 MB, Pharmacia). The column material was equilibrated in a sodium phosphate buffer (15 mM, pH 7.2) containing 0.05% deoxycholate, 0.025% NaN_3 and 0.25 M NaCl. The glycophorin-loaded column was washed with buffer (five times the column volume) and the protein was then eluated by 0.1 M *N*-acetylglucosamine in phosphate buffer. The solution was dialyzed several times against distilled water and freeze dried. SDS gel electrophoresis of the purified protein showed one band at 65 kDa which corresponds to the molecular weight of the glycophorin dimer [11].

Glycophorin was incorporated into DMPC bilayers according to Mac Donald and Mac Donald [12]. The lipid was dissolved in a methanol/chloroform mixture (3:1, v/v). Glycophorin was added from a solution in pure water (10 mg/ml) mixed in an appropriate amount* to adjust the lipid to protein ratio. Slight sonification in a bath sonifier was applied. The mixture was dried to a thin film in a 100 ml flask under vacuum. In order to remove residual methanol the flask was kept in a dessicator overnight. The film was swollen for 1 h in a wet atmosphere and then carefully removed from the glass wall with Tris-HCl buffer (0.1 M, pH 7.5). As determined by electron microscopy thin-walled vesicles with an average diameter of 0.5–1 μm were formed. The values of the protein concentration may exhibit a relative error of about 20%.

Freeze-fracture electron microscopy

Thin layers of the vesicle suspensions kept between gold plates (0.7 mm thickness) were rapidly frozen in Freon (−155°C). In order to obtain reproducible freezing rates the layer thickness was kept constant by intercalating 20-μm thick EM-grids between the gold plates. Before freezing, the preparations were equilibrated at the desired temperature for 16 h. Freeze-fracturing was performed in a Balzers BAF 400 D at −120°C and 10^{-7} mbar without special etching. Platinum/carbon shadowing was applied.

Differential thermal analysis

Calorimetric studies were performed with a commercial micro-calorimeter (Triflux Thermanalyse). Samples containing about 10 mg of lipid in 400 μl of water brought to pH 7.5 were studied. The exact amount of lipid was determined after

* The protein concentration is given in ‰ corresponding to the mol fraction of monomeric glycophorin with respect to the total amount of lipid and protein throughout the paper.

the measurements by weighing the freeze-dried samples. The calorimetric curves were normalized to the same amount of lipid. The heating rate was 0.2 K/min and the cooling rate 0.1 K/min.

Energy-transfer experiments

Fluorescein was used as energy donor and eosine as acceptor. Glycophorin was labeled with isothiocyanate derivatives of these dyes. The protein was incubated with a 100-times molar excess of the isothiocyanates for 4 h at 4°C in a 0.1 sodium borate buffer adjusted to pH 9. The glycophorin was separated from the excess dye on a Sephadex G-5 column and the salt was removed by dialysis. Absorbance measurements showed an average labeling of one dye molecule per protein. Electrophoresis of the fragments after trypsin treatment showed a fluorescent band only for the sugar containing headgroup [1]. Dimyristoylphosphatidylethanolamine was labeled in the same manner. Fluorescence measurements were performed with a Schoeffel spectrofluorimeter RRS 1000 in 4 mm microcuvettes. Fluorescein was excited at 440 nm in order to minimize the direct acceptor absorption. For all measurements the total emission spectra were recorded between 460 nm and 660 nm. For the evaluation of the energy transfer efficiency, corrected fluorescence intensities of the donor (F_{DA} at 518 nm) and the acceptor (F_{AD} at 550 nm) were used. These values were obtained by subtracting the residual fluorescence intensities of the donor at 550 nm from the measured values F_A and that of the acceptor at 518 nm from the value F_D. All glycophorin molecules were labeled. The ratio of acceptor and donor was 1:1 which was also valid for the lipid probes. The dye concentration with respect to the water was about 10^{-7} M. However, its accurate value in the measured preparation is difficult to keep constant due to the losses of lipid and incorporated dyes. Under the assumption that the initial composition of the vesicles (lipid to dye ratio) does not change during the preparation, the following evaluation procedure can be applied:

The fluorescence intensity of the donor in the presence of the acceptor is given by Eqn. 1a [13]

$$F_{DA} = \epsilon(\lambda_e) \cdot I_0 \cdot x_D \cdot l \cdot d \cdot f(\lambda_D) \cdot \varphi_{DA} \qquad (1a)$$

where $\epsilon(\lambda_e)$ is the extinction coefficient and I_0 the intensity of the exciting wavelength λ_e. x_D is the donor concentration, l the microcuvette length, φ_{DA} the quantum yield of the donor in the presence of the acceptor and $f(\lambda_D)$ the fraction of radiation emitted at λ_D. d is a constant of the detector depending on geometry and wavelength.

The energy transfer efficiency which is a function of the acceptor concentration is given by $E = 1 - \varphi_{DA}/\varphi_D$ where φ_D is the quantum yield of the donor in the absence of the acceptor. The number of excited acceptor molecules is given by $x_D \cdot \epsilon(\lambda_e) \cdot I_0 \cdot l \cdot E$ which means that the acceptor's fluorescence is

$$F_{AD} = x_D \cdot \epsilon(\lambda_e) \cdot I_0 \cdot l \cdot E \cdot d \cdot f(\lambda_A) \cdot \varphi_A \qquad (1b)$$

φ_A is the acceptor's quantum yield in the absence of the donor and $f(\lambda_A)$ the fraction of radiation emitted at λ_A. Since λ_D and λ_A are neighbouring wavelengths we can use the same detector constant d for F_{DA} and F_{AD}. Under the assumption that $f(\lambda_A) \cdot \varphi_A \cong f(\lambda_D) \cdot \varphi_D$ the energy transfer efficiency is approximately given by

$$E \cong \left(1 + \frac{F_{DA}}{F_{AD}}\right)^{-1} \qquad (2)$$

The ratio F_{DA}/F_{AD} is independent of the vesicle concentration and insensitive to scattering effects. However, it depends strongly on the dye concentration within the vesicles and can thus give insight into the molecular arrangement.

EPR-measurements

Spin-labeled fatty acid I (12, 3) obtained from Syva (Palo Alto, CA) was added to the initial methanol-chloroform solution of lipid and protein to come to 1% with respect to the lipid. Reconstitution of protein containing vesicles was performed as described above. The vesicles were centrifuged at $10000 \times g$ and 10 μl of the pellet were transferred into an EPR tube. Spectra were recorded with a Varian E-4 spectrometer.

Fluorescence recovery after photobleaching (FRAP) technique

Protein diffusion coefficients D were measured by the FRAP technique introduced by Peters et al. [14] using the evaluation procedure of Axelrod et al. [15]. The apparatus used in the present work

has been described earlier [16]. Large protein-containing vesicles were directly prepared on microslides at 30°C by swelling thin films obtained as described above. Vesicles were formed spontaneously upon addition of phosphate buffer (phosphate buffered saline at pH 7.5). The specimens were sealed under coverglasses and equilibrated for at least 10 h before the measurements. By this procedure mechanical stresses were reduced to such an extent that vesicles up to 50 μm diameter were obtained.

Bleaching experiments were performed on thin-walled vesicles using the fluorescence intensity as an indicator for wall thickness. For each selected temperature and concentration three to five vesicles were measured. The bleaching spot size was 5 μm.

Results

Differential thermal analysis

Fig. 1 shows the variation of heating and cooling curves of DMPC vesicles as a function of glycophorin concentration, x_p, given in mol‰. The pretransition is only observed in the heating curve at $x_p = 0$. The absence of the pretransition upon cooling is a common finding. The arrows indicate the temperatures of onsets of lipid phase-transitions. The onset temperature of the heating curves is shifted from 21.5°C at $x_p = 0$‰ to a constant value of 20°C between 0.7‰ and 2.6‰ and decreases further above $x_p = 3.4$‰. The transition curves are slightly broadened up to 2.6‰ with a maximum width at $x_p = 0.7$‰. Above 3.4‰ they seem to consist of a rather sharp peak superimposed on a broad component. For evaluation the onset temperature (liquidus line) was obtained by extrapolation of the sharp peak as indicated by the dashed line.

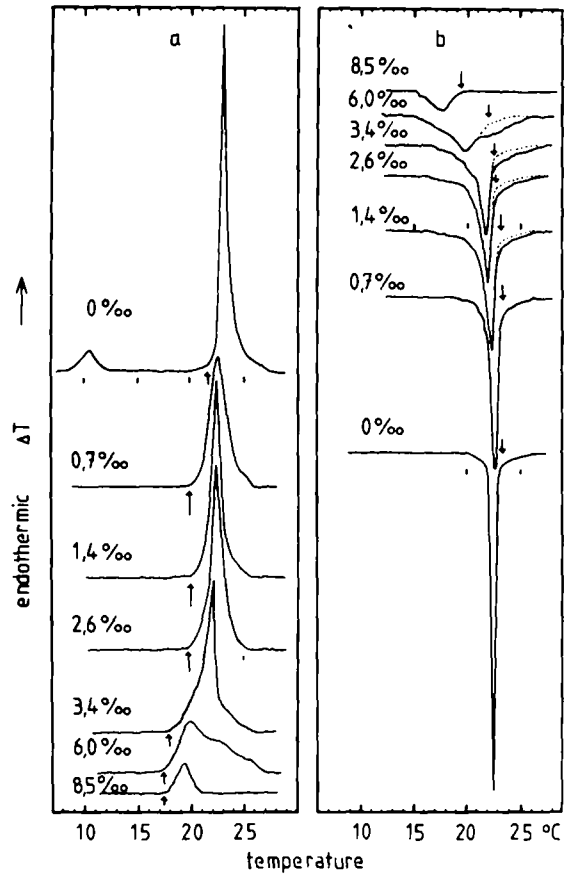

Fig. 1. Differential thermal analysis curves of DMPC vesicles containing different glycophorin concentrations. (a) Heating curves at 0.2 K/min. (b) Cooling curves at 0.1 K/min. All curves are normalized to the same amount of lipid. The arrows indicate the temperatures of the onset of the lipid phase transitions. In the case of the cooling curves they are obtained by extrapolating the dashed lines.

Electron paramagnetic resonance

Fig. 2a shows the order parameter of a fatty acid spin label both as a function of temperature and protein concentration. All curves exhibit a minimum at $x_p = 0.8$‰.

While the minimum is shallow well above the main transition (23°C) and below the pretransition, it is rather deep between the two transitions, that is within the temperature region of the P_β phase. The phase transition temperatures of glycophorin containing vesicles obtained from the order degree measurements are shown in Fig. 2b as a function of the glycophorin concentration. A minimum in the phase transition temperature is observed at 0.8 mol‰ of glycophorin.

Diffusion measurements

The vesicles studied were homogeneous within the dimensions of the optical resolution (0.2 μm). Lateral mobilities over distances of μm were measured.

Above the main phase transition temperature,

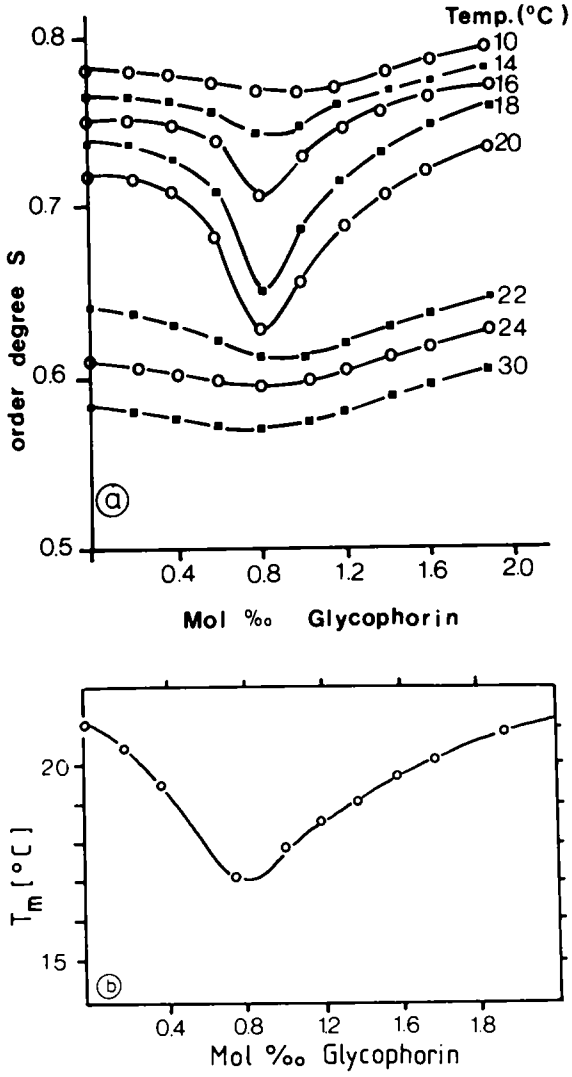

Fig. 2. (a) The order parameter, S, of the lipid phase as obtained from the EPR spectra of spin-labeled fatty acid (I(12, 3)). S is plotted as a function of glycophorin concentration for different temperatures. (b) Apparent transition temperature of DMPC vesicles in the presence of different amounts of glycophorin as obtained from the plots of S versus T.

T_m, the diffusion coefficient, D, does not depend on the protein concentration at least up to 2‰ within the accuracy of measurement. At 30°C one observes an average value of $4 \cdot 10^{-8}$ cm^2/s while D varies exponentially with temperature. Below T_m the temperature dependence of the diffusion coefficient varies in a characteristic way with the concentration. Below the pretransition temperature, T_p, strong kinetic effects are observed.

D versus temperature plots for three characteristic protein concentrations are given in Fig. 3.

(a) At $x_p = 0.4$‰ (Fig. 3a) the temperature dependence of D shows only a break at the main transition temperature T_m and D decreases nearly exponentially with T by about a factor of ten between T_m and T_p. If the latter temperature is reached, D drops abruptly and two fractions of different mobilities coexist: a mobile fraction with $D = 5 \cdot 10^{-10}$ cm^2/s and a completely immobilized one with $D < 10^{-11}$ cm^2/s. Strong hysteresis effects are observed below T_p. This behaviour is characteristic for protein concentrations up to $x_p = 0.5$‰.

(b) At $x_p = 0.9$‰ (Fig. 3b) the diffusion coefficient exhibits an essentially different temperature dependence. At 20°C, D drops abruptly by a factor of 15. Note that this slowing down involved all molecules simultaneously. This is clearly demonstrated by the fact that the fluorescence recovery curves agree well with the theoretical curve determined by only one recovery time. Below 18°C we observed splitting into two fractions characterized by $D \cong 10^{-9}$ cm^2/s and $D < 10^{-11}$ cm^2/s.

(c) At 3.2‰ (Fig. 3c) D decreases exponentially from $D = 4 \cdot 10^{-8}$ cm^2/s at $T = 30$°C to $D = 2 \cdot 10^{-8}$ cm^2/s at 17°C. Thereafter D decreases much faster in a broad transition region to about 10^{-9} cm^2/s.

Freeze-fracture electron microscopy

Figs. 4 and 5 show a series of freeze-fracture electron micrographs of glycophorin-containing DMPC vesicles. The texture of the $P_{\beta'}$ phase at 19°C depends in a characteristic way on the glycophorin concentration:

(1) At $x_p < 0.2$‰ (Fig. 4a) the texture strongly resembles that of the $P_{\beta'}$ phase of pure DMPC. The ripples are clearly asymmetric which is due to a sawtooth-like cross-section. The period is 120 Å. This is characteristic for one of the two possible $P_{\beta'}$ phases which has been reported previously and is denoted as $\Lambda/2$ phase [17]. A characteristic feature of this phase is the appearance of line defects occurring where two regions of opposite ripple orientation meet. The end points of the line defects denoted by $\pm 1/2$ are analogous to the point defects of the second type of $P_{\beta'}$ structure

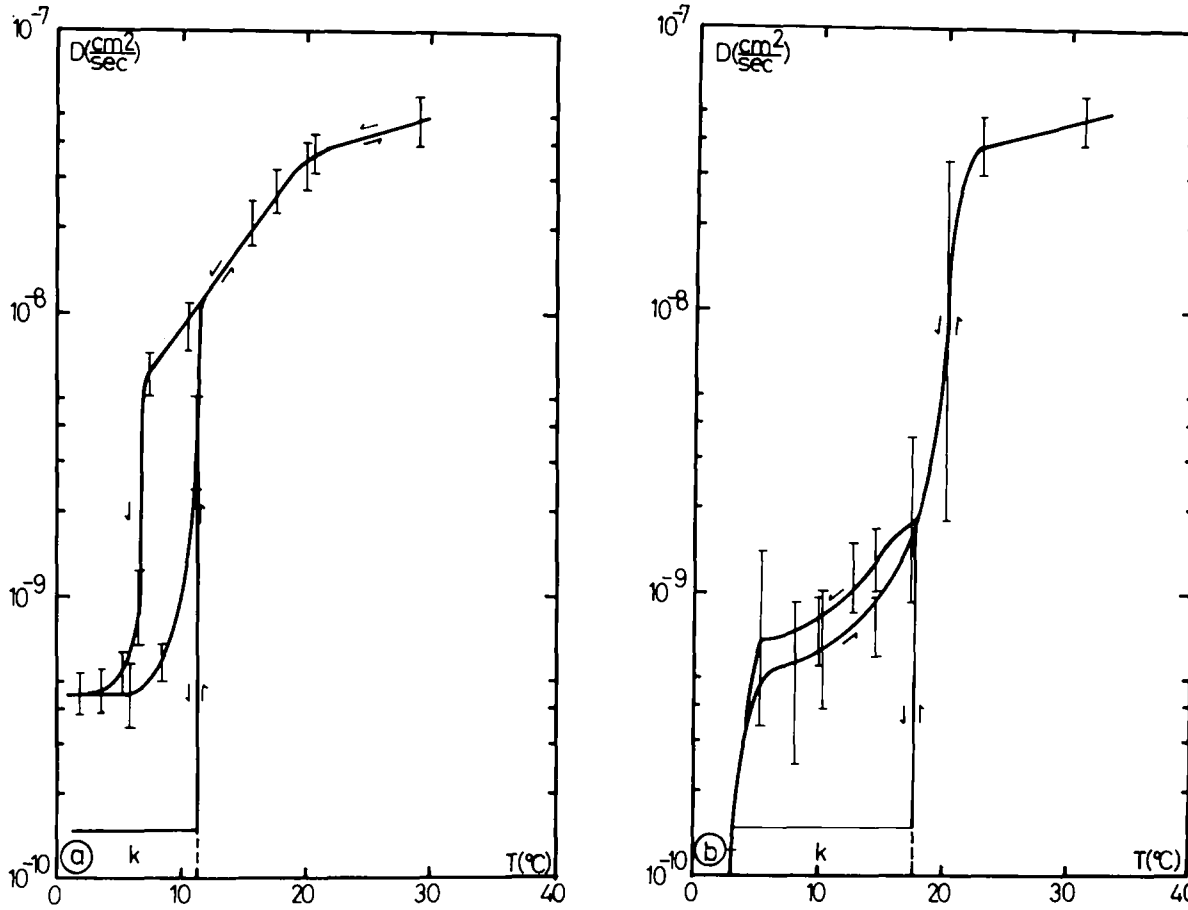

Fig. 3. (a) and (b).

called Λ phase [17]. A closer inspection shows that the line defects are laterally expanded and simultaneously shortened in comparison to the Λ/2 phase of pure DMPC which may be due to an accumulation of the protein in these regions of distorted lipid structure. This is in agreement with the observed influence of cholesterol on the $P_{\beta'}$ ripple phase [17] and thus seems to be a general effect of impurities on the ripple structure. Small vesicles exhibit a polygonal shape. The planes of these are made up of pure crystalline lipid while the edges are formed by the expanded defect lines.

(2) At $x_p = 0.4‰$ (Fig. 4b) a domain-like structure appears which consists of islands (R) of the regular Λ/2 phase and regions of an irregular ripple structure (I). The latter replace the expanded defect lines and contain the glycophorin.

(3) At increasing protein concentration the colonies of irregular ripple structure (I) grow at the cost of the Λ/2 phase (R). At about $x_p = 0.8‰$ the latter has nearly vanished (Fig. 4c).

(4) At $x_p = 1.2‰$ (Fig. 4d) a regular Λ phase reappears again and grows in area with increasing protein concentration. Note that the direction of the ripples and the interripple distance fluctuate.

(5) Above about $x_p = 1.7‰$ the regular ripple phase disappears again and is completely absent at $x_p = 2.0‰$.

To test whether the disappearance of the regular ripple structure is caused by the interaction of

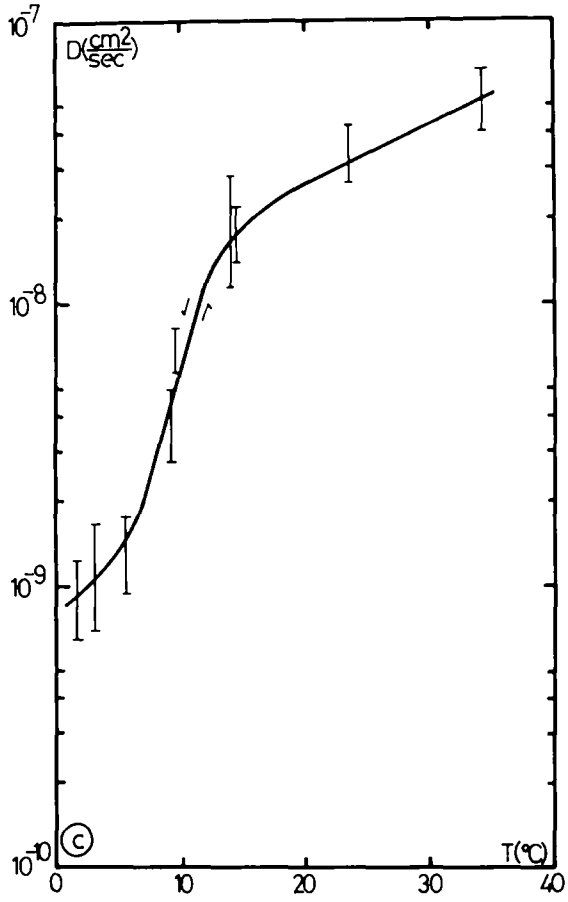

Fig. 3. The temperature dependence of diffusion coefficient D of glycophorin in DMPC vesicles for protein concentrations of (a) 0.4‰, (b) 0.9‰ and (c) 3.4‰.

the lipid with the sugar containing headgroup, these were removed by trypsin treatment of the reconstituted DMPC-glycophorin vesicles. According to Fig. 5d the regular Λ-ripple phase is restored.

Special attention was paid to the appearance of particles. In the fluid phase no particles were observed at least up to $x_p = 10‰$. At low temperatures (e.g. 4°C) particles appeared above $x_p = 1‰$ (Fig. 5a). The particles are preferentially located in the line defects. It should be noted that at 4°C a ripple phase is observed for glycophorin concentrations higher than 0.4‰. At lower concentrations the vesicles exhibit a nearly smooth surface which is characteristic for pure DMPC equilibrated for several hours.

Energy transfer experiments

So far we had not obtained any information about the microstructure of the DMPC-glycophorin model membranes above the main transition temperature. Therefore, the energy transfer was studied between dyes attached to glycophorins as well as between dyes attached to the lipids.

Dimyristoylphosphatidylethanolamine was used as lipid probe in order to minimize disturbance of the lipid structure. The energy transfer between lipids was studied as an example for a random distribution of probe molecules in the plane of the membrane.

The results are shown in Fig. 6. The ordinate is given by $(1 + (F_{DA}/F_{AD}))^{-1}$. F_{DA} and F_{AD} are the corrected values of the maximum fluorescence intensities of the donor (fluoresceine) in the presence of acceptor, and of the acceptor (eosine) in the presence of the donor, respectively (cf. insert of Fig. 6). According to Eqn. 2 the ordinate is a direct measure of the energy transfer efficiency. It exhibits the following features:

(1) The lipid-to-lipid transfer efficiency shows an s-like curve which is characteristic for randomly distributed donors and acceptors. (Only the lower half of the s-curve is shown.)

(2) The protein-to-protein transfer shows a peculiar behaviour. It increases abruptly at a protein concentration of 0.5‰, reaches a maximum at 1.2‰ and decreases again to a minimum value at 3.5‰. Above this concentration the efficiency coincides with that of the lipid-to-lipid transfer.

Discussion

A number of different techniques have been applied in order to gain insight into the microstructure of the DMPC-glycophorin model membranes. The main emphasis was directed towards low protein concentrations ($x_p < 1\%$). We have considered glycophorin as a monomer although it is known to exist as a dimer in SDS. Segrest [18] has developed a hexamer model for the trypsinated T(is) hydrophobic helical core of glycophorin. However, at low protein concentrations ($x_p < 1\%$) he assumes that even the trypsinated peptide exists as a monomer in bilayer lipid membranes. For the intact glycophorin we expect an even higher critical multimer concentration due to the bulky

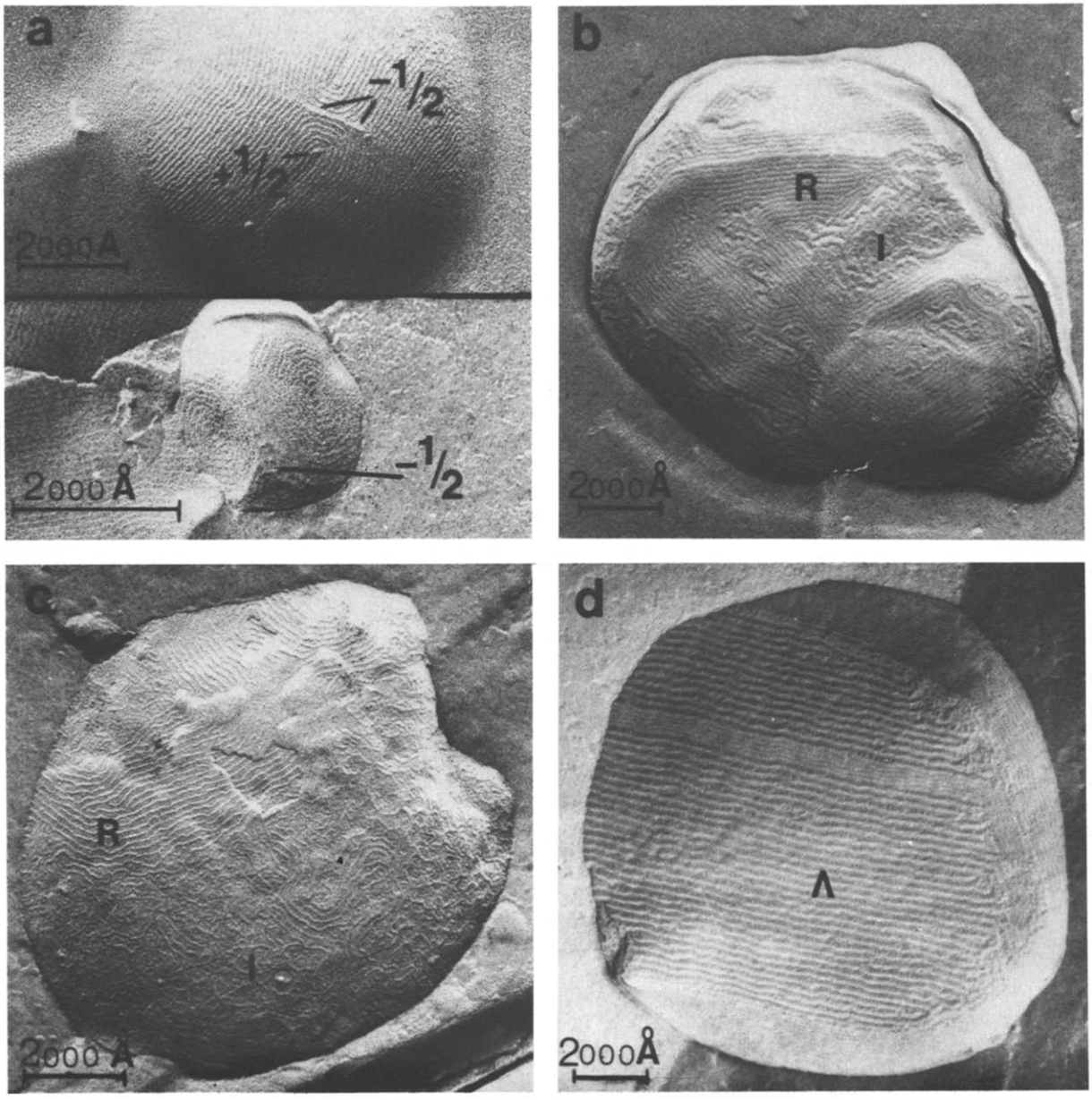

Fig. 4. Freeze-fracture electron micrographs of DMPC vesicles containing variable amounts of glycophorin frozen from 19°C. (a) $x_p = 0.2‰$. A section of a large vesicle (about 1 μm diameter upper picture) and a small vesicle (about 0.1 μm diameter, lower picture) are shown. (b) $x_p = 0.4‰$. (c) $x_p = 0.8‰$. (d) $x_p = 1.3‰$.

headgroup. Moreover, from our diffusion measurements, in comparison to the lipid diffusion, we can exclude at least tetrameric forms.

Our experiments lead to the conclusion that $x_p = 0.8‰$ is an important protein concentration. In the following discussion we shall interpret this point as the beginning of a conformational change in the glycophorin headgroup area.

As mentioned in the results section, the 0.8‰ concentration is distinguished by a maximum broadness of the heating curve in the concentration range between 0 and 2.6‰. This may be

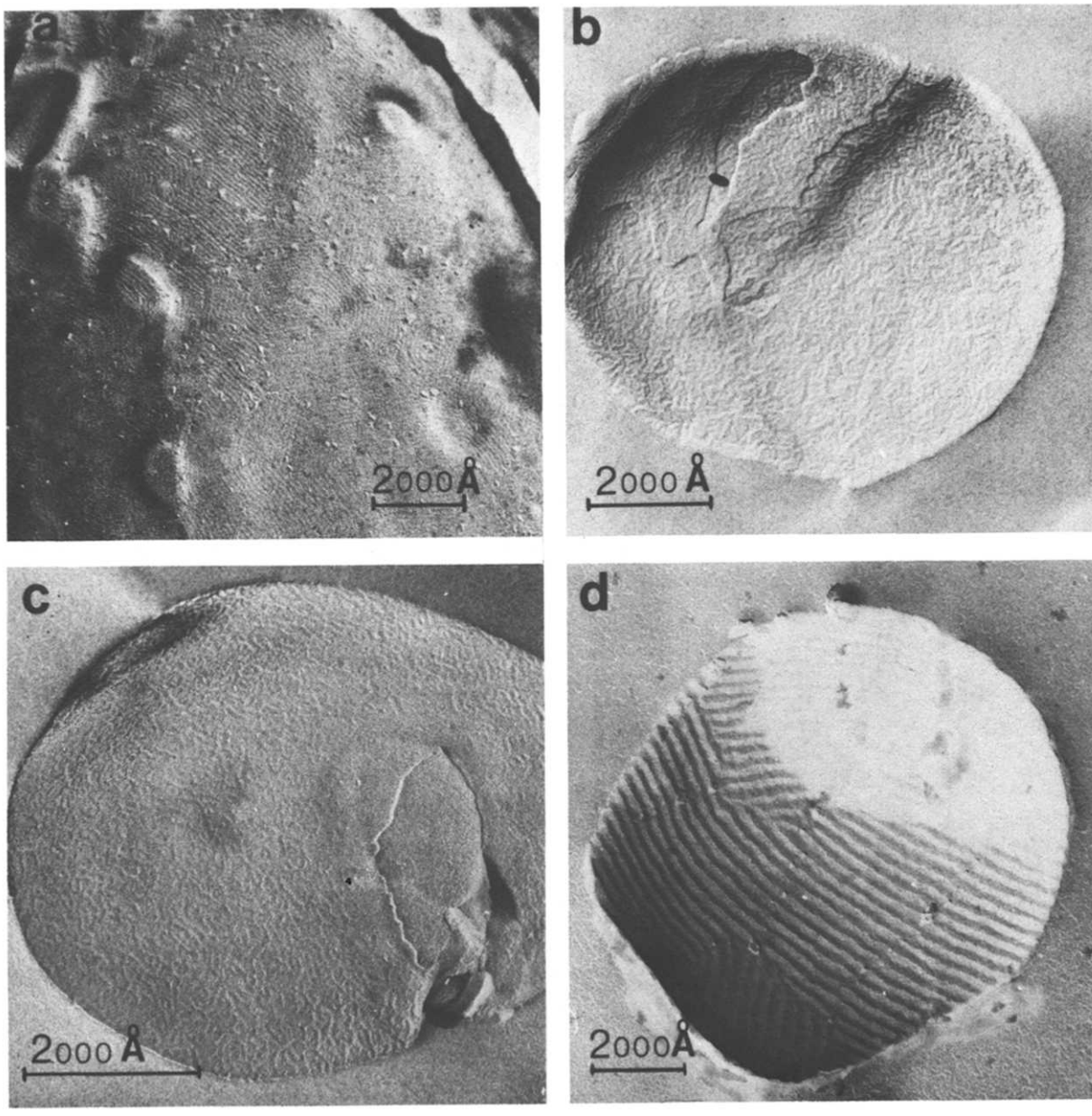

Fig. 5. Freeze-fracture electron micrographs of DMPC vesicles containing (a) 8‰ glycophorin at 4°C, (b) 5‰ at 19°C and (c) 8‰ at 37°C, (d) reappearance of the ripple phase at 19°C caused by trypsin treatment of the preparation shown in Fig. 5b.

interpreted in terms of a minimum lipid cooperativity corresponding to a maximum number of lipid molecules coupling to the protein. The onset temperatures of the heating and cooling curves define the solidus and the liquidus lines of the binary DMPC-glycophorin mixture. The phase boundary lines are plotted in the tentative phase diagram of Fig. 7.

The total areas under the calorimetric curves obtained from Fig. 1 are plotted in Fig. 8 as a function of x_p. Above 1.4‰ only the areas under the dashed lines are considered. A nearly horizon-

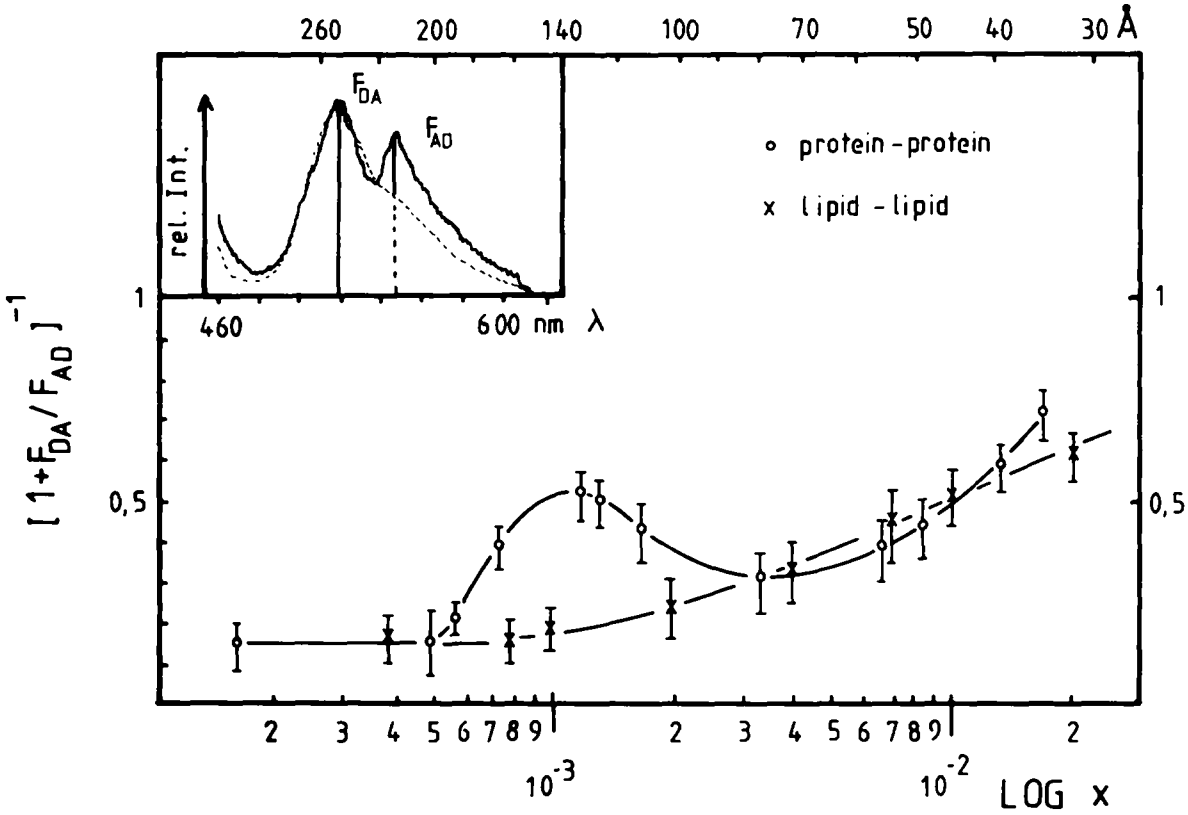

Fig. 6. Energy transfer efficiency in DMPC-vesicles at 37°C as a function of the total concentration, x, of dye-labeled probe molecules. F_{DA} and F_{AD} are defined in the insert. The curve (× ——— ×) gives the result for the energy transfer between dyes attached to dimyristoylphosphatidylethanolamine (lipid-lipid transfer). The curve (○ ——— ○) holds for the energy transfer between dyes attached to glycophorin (protein-protein transfer). x stands for the total protein concentration in the case of protein-protein transfer, and for the total lipid label in the case of the lipid-lipid transfer. The upper abscissa gives the average distance between glycophorin molecules or lipid labels.
(Insert) Full line: total emission spectrum of DMPC containing $x_p = 2‰$ lipid dyes. In the overlapping region the course of the emission spectrum of the pure donor is indicated by the broken curve.

tal deflection is observed between $x_p = 1.4‰$ and $x_p = 3.4‰$ in close similarity to the behaviour of the solidus line. These areas are proportional to the enthalpy changes during the lipid phase transition.

Provided it is not influenced by the lipid-protein interaction, the areas correspond to the fraction of lipid free to undergo the main phase transition.

The ΔH versus x_p curves exhibit two linear regions, AB for low and CD for high concentrations. If one extrapolates these straight lines to $\Delta H = 0$ one obtains the number N of lipids interacting with one protein. For the small concentrations one gets $N = 300$ and for the high concentration region $N = 100$. The latter value is in agreement with the findings of van Zoelen et al. [6]. The two different numbers of lipids interacting with one protein suggest that the glycophorin may occur in two different states. As will be shown below, this two-state model is the basis of the understanding of the energy transfer experiments.

The spin label results also exhibits interesting behaviour at the critical protein concentration of $x_p = 0.8‰$. Here the order parameter at temperatures well below the main transition (that is at least down to 18°C) is as low as above the phase transition (23°C) in the absence of protein. A comparison with the diffusion measurements (Fig. 3) shows that this is indeed due to a lipid

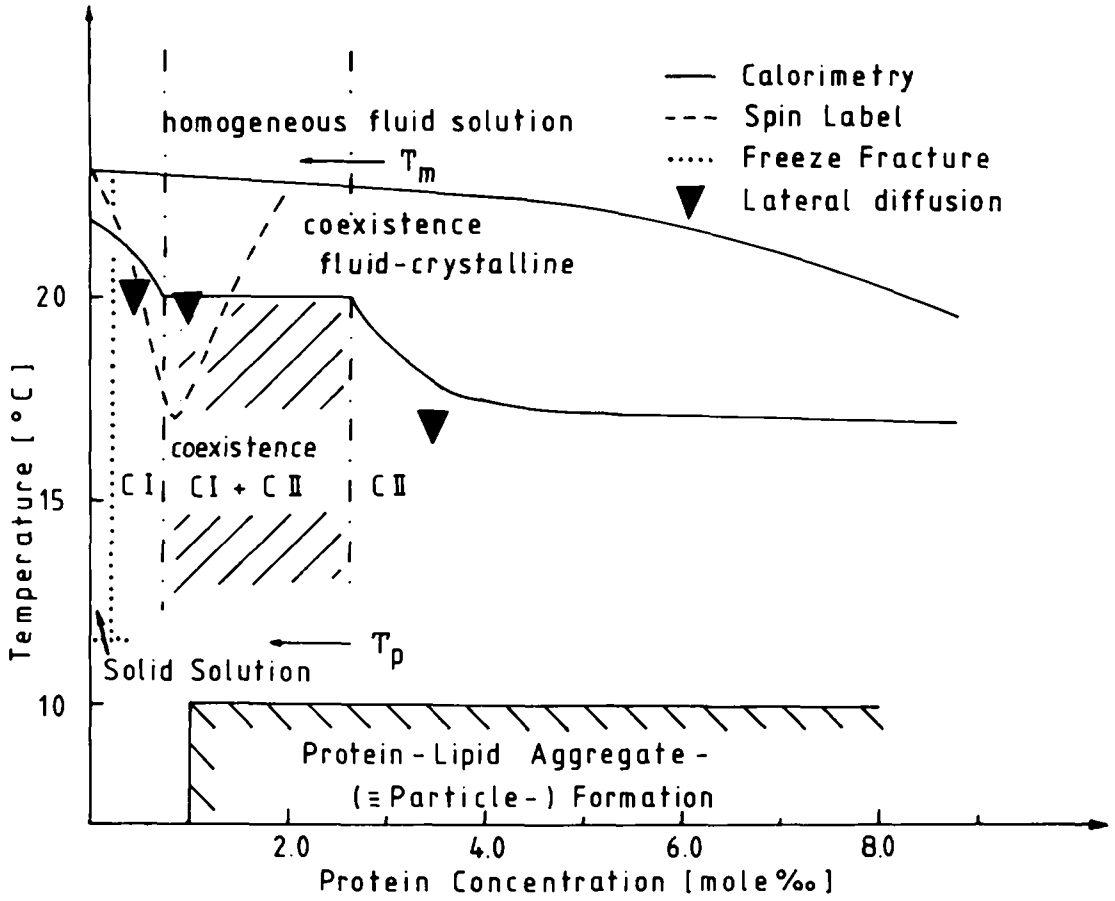

Fig. 7. Tentative phase diagram of the binary system glycophorin/DMPC combining the results from calorimetry (———), spin label study (------), electron microscopy (· · · · · ·) and lateral diffusion measurement (▼). CI describes the pancake-like conformation I and CII the three-dimensional conformation II.

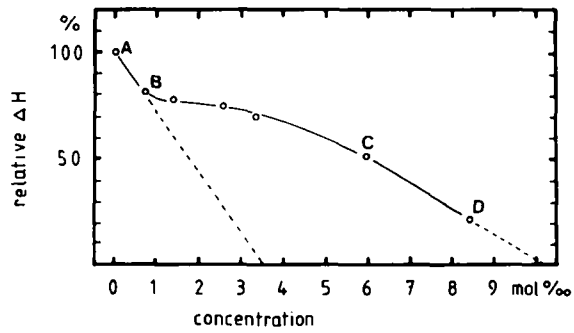

Fig. 8. Relative transition enthalpies ΔH obtained by integration of the calorimetric cooling curves of Fig. 1. Only the area under the extrapolated dashed lines has been considered.

fluidization. The apparent transition temperatures shown in Fig. 2b are represented in the tentative phase diagram of Fig. 7. At low concentrations good agreement with the solidus line obtained from calorimetry is observed.

The ascending branch of the broken curve is in contrast to the calorimetric result. This may be explained in terms of phase separation which leads to superposition of different spectra. This makes it impossible to determine phase transitions in a reliable way. According to Fig. 2 the concentration dependence of the order parameter exhibits a shallow minimum at the specific concentration of 0.8‰ both above the main ($T > 23$°C) as well as below the pretransition ($T < 14$°C) temperatures. As known from molecular statistical theories [19] the

order parameter is a measure for the lateral packing density of the lipid molecules. This leads to the conclusion that at $x_p = 0.8‰$ the lipid-protein coupling is most effective, thus leading to a decoupling of the lipid-lipid interaction.

The concentration dependence of the protein-to-protein energy transfer exhibits three features. Firstly, the steep increase of the transfer efficiency, E, at an astonishingly low concentration of the dye-carrying molecules. Secondly, the following decrease in E at increasing concentration. Finally, the coincidence of the E versus x_p curve at high concentrations with that characteristic for a random distribution of small rigid donors and acceptors.

We considered two explanations for this peculiar behaviour: (1) an aggregation of the proteins or (2) a change of the protein headgroup conformation. We discarded the first possibility for the following reasons. An aggregation of proteins at low concentration would lead to a saturation behaviour with E = constant at $x_p > 1‰$. The decrease in E above 1.3‰ of protein and the statistical behaviour at $x_p > 3.5‰$ does not fit such a model.

The energy transfer experiments may be explained in terms of the second picture. We propose a model based on the assumption that the sugar-containing protein headgroup may exist in two conformations: (1) in a flat (pancake like) structure where the headgroup forms a nearly two-dimensional layer spread on the membrane surface (conformation I); and (2) in an upright conformation (conformation II) in which the headgroups protrude out into the aqueous phase, that is into the third dimension (fig. 9). For steric reasons conformation I can only exist at low protein concentrations while the erected head group conformation II is expected to prevail at high concentrations since it allows a higher protein packing density.

The energy transfer efficiency for an arrangement of donors and acceptors in the plane of the membranes has been calculated numerically by Dewey and Hammes [20]. These authors extended the Förster theory to the case of a statistical distribution of acceptors and donors in a two-dimensional plane. We can apply their numerical integrations because our vesicles are very large. For our purpose the protein concentrations have been divided into three regions: (1) $0 < x_p \leq 0.8‰$: proteins exist in the flat structure I; (2) $0.8 < x_p < 3.2‰$: coexistence of conformations I and II; (3) $x_p \geq 3.2‰$: all proteins in conformation II. The concentration limits $x_p = 0.8‰$ and $x_p = 3.2‰$ are suggested by the end points of the horizontal line in the phase diagram (Fig. 7). Moreover, they lead to the best fit between the experimental and the calculated E versus x_p curve. The three concentration regions will be discussed in the following sections.

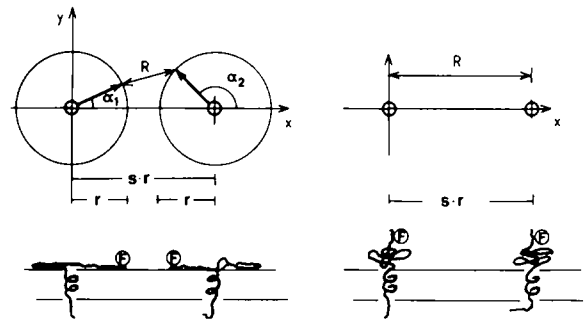

Fig. 9. Calculation of energy transfer. Relative position of chromophores, F, for the structures I (left side) and II (right side), respectively. r is the distance of the chromophores from the axes of the α -helices. The distance between the α-helix axes $s \cdot r$ is given in units of r.

(a) Region $o < x_p \leq 0.8‰$ (cf. Fig. 9, left side).

The rate of energy transfer between two dyes is given by the Förster equation

$$\kappa = \frac{1}{\tau}\left(\frac{R_0}{R}\right)^6 \tag{3}$$

where R_0 is the Förster radius and τ is the life time of the excited donor in the absence of energy transfer. Now the helices of glycophorin are randomly distributed in the plane of the membrane. The fluorophores of a donor-acceptor pair are fixed on circles of radius r around the helices while the angles α_1 and α_2 are randomly distributed.

The random distribution of angles can be incorporated into a modified Förster equation by integrating over all possible pairs (α_1, α_2). It should be noted that at small distances of the helices the energy transfer rate becomes extremely large if $\alpha_1 = 0°$ and $\alpha_2 = 180°$ and the contributions of all

other (α_1, α_2) pairs can be neglected. Following the same procedure as applied by Dewey and Hammes [20] in the derivation of their equation (30) we obtain

$$\kappa' = \frac{1}{\tau}\left(\frac{R_0}{r}\right)^6 \frac{s^6 - 2s^4 + (8/3)s^2}{(s^4 - 4s^2)^3} \tag{4}$$

where $s \cdot r$ is the distance of the α-helices. By introducing an effective Förster radius R_{eff} according to

$$R_{eff}^6 = R_0^6 \frac{s^6 - 2s^4 + (8/3)s^2}{(s^4 - 4s^2)^3} \tag{5}$$

one obtains Eqn. 3 where R_0 is replaced by R_{eff}. The transfer efficiency, E, is now obtained as a function of the acceptor surface density σ by replacing R_0 by R_{eff}. Best fit is obtained for $R_{eff}/L = \infty$ in the whole concentration region and for $s = 2.19$ at $x_p = 0.8‰$. L is the nearest approach of donors and acceptors. The fitted curve is shown in Fig. 10 together with the experimental values.

(b) Region $x_p \geq 3.2‰$ (cf. Fig. 9, right side)

In this region the transfer efficiency curve agrees to a good approximation with that of the lipid-to-lipid energy transfer (cf. Fig. 6). It is $E = 0.5$ for $x_p = 10‰$ corresponding to an average lipid distance of 47 Å which in this case is equal to the Förster radius R_0. This value of R_0 corresponds then to $E = 0.5$ if the adaptable parameter R_0/L is $R_0/L = 1.3$. The calculated E versus x_p curve (at $x_p \geq 3.2‰$) is given in Fig. 10.

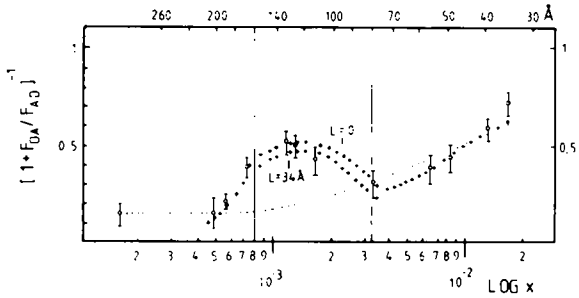

Fig. 10. Comparison of calculated (+) and experimental efficiency (O) of protein-protein energy transfer. L is the nearest approach of the donor and the acceptor. Three regions of protein concentration are indicated:
(a) 0–0.8‰ where protein headgroups are assumed to lie flat on the membrane surface (pancake conformation I; $L = 34$ Å).
(b) 0.8–3.2‰: coexistence of conformation I and II (fitted curves for $L = 0$ and $L = 34$ Å are shown). The broken line gives the experimental lipid-lipid energy transfer.

(c) Region $0.8 < x_p \leq 3.2‰$

This is a very complicated situation since three types of donor-acceptor pairs (I-I, I-II and II-II) are possible. For simplification the donor-acceptor pair I-II is not considered and we assume that all proteins form either I-I or II-II pairs. This leads to a tolerable estimation of the transfer efficiency.

The fraction x_{II} of proteins in conformation II is assumed to vary in a linear manner between the concentration limits (0.8‰ and 3.2‰), that is

$$x_{II} = \frac{(x_p \cdot 10^3) - 0.8}{2.4} \tag{6}$$

The transfer efficiency is determined by an effective Förster radius

$$R^*_{eff} = (1 - x_{II})R_{eff} + x_{II}R_0 \tag{7}$$

where the value of R_{eff} obtained for $x_p = 0.8‰$ has to be taken: $R_{eff} = 110$ Å. The efficiency E has been obtained as above. This has been done for $L = 0$ (upper curve in region 2 of Fig. 10) and for $L = 34$ Å (lower curve of Fig. 10). Obviously the value of L does not have a strong influence. According to the work of Fung and Stryer [21] the transmembrane energy transfer can be neglected in a first approximation.

Structural information from the electron microscopic study is only obtained below the main phase transition. The results presented in Fig. 4a suggest that up to $x_p = 0.2‰$ the glycophorin-DMPC system forms a solid solution. Since the α-helix of the protein occupies a 3-times larger area than the lipid it is preferentially incorporated into the cores of the point and line defects. The proposed microstructure is presented in Fig. 11. The protein containing islands are non-crystalline. This is suggested by the fact that they form the soft edges of the polygonal-shaped vesicles (Fig. 4a, lower part). Above the solubility limit of $x_p = 0.2‰$ further addition of the protein causes phase separation leading to a domain-like structure of the regular $\Lambda/2$ phase and the irregular ripple structure (Fig. 4b). The proposed microstructure is

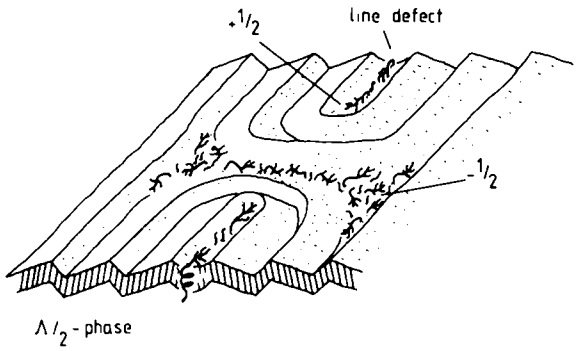

Fig. 11. Proposed microstructure of glycophorin-DMPC bilayers in the $P_{\beta'}$ phase at protein concentrations below the solubility limit. The protein accumulates preferentially in line defects and point defects. The defect cores expand by the protein incorporation.

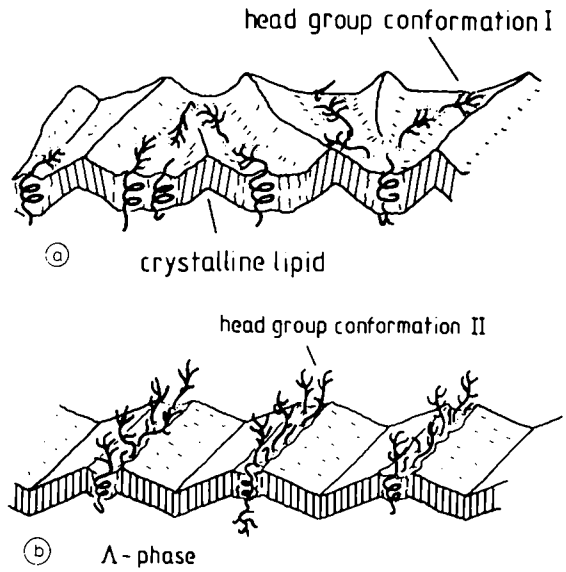

Fig. 12. Proposed microstructure of glycophorin in DMPC at 19°C ($P_{\beta'}$ phase) at protein concentrations above the solubility limit. (a) Irregular ripple structure at the critical protein concentration of $x_p = 0.8‰$. The structure is typical for $0.2 \leq x_p \leq 10‰$ where the sugar-containing protein headgroup is supposed to assume a flat structure I. The ripples are attributed to crystalline lipid, the flat islands to protein-saturated lipid. (b) Microstructure typical for $1‰ \leq x_p \leq 2‰$ with proteins in headgroup structure II (raised headgroup). The case of Λ ripples is shown.

shown in Fig. 12a. The dam-like structures of the irregular ripple phase are interpreted as pure crystalline lipid. This is consistent with our calorimetric finding that 80% of the lipid takes part at the main phase transition. A most puzzling result is the disappearance of the regular ripple phase at the distinguished concentration ($x_p = 0.8‰$) and its reappearance at a slightly higher concentration ($x_p \cong 1.2‰$). While the $\Lambda/2$ phase prevails at low concentrations, the Λ phase dominates in the reappearing ripple structure. However, compared to the situation of the $P_{\beta'}$ phase of pure DMPC the direction of the Λ ripples as well as their mutual distance fluctuate considerably. Together with the absence of the irregular ripple structure the above distortion leads to the conclusion that the protein is to a large extent incorporated into the Λ ripples. Obviously it is for this reason that the $\Lambda/2$ phase disappears in favour of the Λ phase. The striking difference between the microstructures found for $x_p = 0.8$ and $x_p = 1.2‰$ may be explained on the basis of the two-conformation model suggested by the energy transfer experiments. The lipid in contact with the pancake-forming headgroups does not form ripples while conformation II with its headgroups protruding out into the water phase can be incorporated into the regular ripple pattern. At $x_p = 5‰$ a series of short dams with irregular orientation appears. According to Fig. 7 these are within the coexistence region of fluid and crystalline lipid in agreement with Grant and McConnell [5]. The ripples are most probably formed due to fast phase separation [17] during cooling in the freeze-fracture preparations. In the fluid lipid phase the glycophorin diffusion coefficient is only smaller than that of a lipid probe by a factor of two. As will be discussed in more detail in another paper [22], this shows that D is determined by the lateral motion of the protein moiety buried within the lipid bilayer. The results obtained in the crystalline phase support the interpretations of the results obtained with the other techniques. At $x_p = 0.4‰$ the slow decrease of D below T_m as well as the splitting into a still mobile and an immobile fraction shows that the $P_{\beta'}$ phase exhibits a mosaic-like structure of crystalline islands surrounded by more fluid regions. Some of the latter are large enough to allow for long range diffusion over distances of μm. The immobile fraction may be incorporated into the crystalline islands or may be confined to fluid patches with diameters smaller

than 1 μm. The diffusion is restricted to regions corresponding to areas with the irregular ripple structure visible in the electron micrographs (cf. Fig. 4b). Essentially the same temperature dependence as for 0.4‰ has been found at 0.2 and 0.1‰. According to the freeze-fracture study the protein is then located completely within the expanded defects. Subsequently the line defects may also provide macroscopic paths for fast lateral transport.

At $x_p = 0.9$‰, that is in the neighbourhood of the distinguished concentration, D drops abruptly at $T = 19 \pm 1$°C, that is at the temperature of the horizontal deflection of the solidus line (cf. Fig. 7). As emphasized above, all proteins are slowed down simultaneously and no splitting into two fractions is observed. This is consistent with the electron microscopy finding that all lipid is in the irregular ripple structure at the distinguished concentration and at 20°C. The reduced diffusion coefficient is thus characteristic for the irregular ripple structure. The reduction in D may be caused by the dams of crystalline lipid which form barriers to the protein diffusion so that the effective diffusion lengths of the protein molecules become larger.

At the high protein concentration of $x_p = 3.4$‰ the D versus T curve is characterized by a decrease in mobility within the broad temperature region of 10 K. The upper deflection point at 17°C coincides nearly with the solidus line of the calorimetric studies. This has also been found for the lower concentrations (Fig. 7). The lower deflection point lies in the neighbourhood of the pure DMPC pretransition. The relatively high diffusion coefficient at $T < 5$°C shows that the crystalline phase has an extremely high defect density. As noted above the protein is gradually squeezed out into the water phase.

General discussion

All our experiments suggest that the sugar-containing protein headgroup exhibits two conformations: a quasi two-dimensional pancake structure I and an erected conformation II where the headgroup escapes into the third dimension. The first structure allows for a maximum hydrophilic lipid-protein interaction. The interpretation of the energy transfer results led to the conclusion that conformation II starts to form at the distinct protein concentration of $x_p = 0.8$‰. This suggests that the pancake-like headgroups come into contact. From the relative decrease in the enthalpy of transition (Fig. 8) we obtained the number of lipid molecules interacting with the protein head group conformation I ($N = 300$) and II ($N = 100$). It is intriguing to estimate the maximum number of lipids covered by one protein group on the basis of the Flory-Huggins theory of polymer solutions. The diameters of the two-dimensional structure I (R_I) and the three-dimensional conformation II (R_{II}) are approximately given [23] by

$$R_I = a \cdot n^{3/4} \text{ and } R_{II} = a \cdot n^{3/5}$$

where a is the average length of the monomers and n is the number of monomers. For the sugar-containing headgroup the maximal number of amino acid and sugar monomers is $n \cong 170$. for a value of $a = 3.8$ Å one obtains $R_I \cong 180$ Å and $R_{II} \cong 83$ Å. The estimated areas covered by a headgroup in conformation I or II are then $A_I \cong 25000$ Å^2 or $A_{II} \cong 5000$ Å^2. This corresponds to $N \cong 80$ lipids covered by conformation II and $N \cong 400$ for structure I for an average area per lipid of 65 Å^2. These values of N are consistent with the number of lipids coupling with the protein headgroup as obtained from Fig. 8. It shows that at the distinguished concentration $x_p = 0.8$‰ only 30% of the lipid area is covered by the sugar-containing protein headgroups. According to the lateral diffusion and the calorimetric study the hydrophilic lipid-protein interaction leads to a suppression of the chain melting transition temperature from 22°C to 20°C. This follows from the facts that at $x_p = 0.8$‰: (1) the solidus line starts to become horizontal at 20°C; (2) the lateral diffusion of all glycophorin is reduced by a factor of ten at 20°C; and (3) the enthalpy change of transition is reduced by 20% between $x_p = 0.8$‰ and $x_p = 3.2$‰. The spin label result indicates a suppression of T_m by about four degrees. However, it is well known that this type of spin label indicates a lower transition than the other techniques [24].

The lipid pretransition is very sensitive against the incorporation of glycophorin. The freeze-fracture results show that it vanishes at $x_p \cong 0.4$‰ (Fig. 7). A good indicator for the pretransition is

the vanishing of the well defined (Λ- and $\Lambda/2$-) ripple structure and the appearance of a nearly smooth surface interrupted by a small number of defect lines which is characteristic for the $L_{\beta'}$ phase. At $x_p \cong 0.4‰$ the normal $\Lambda/2$-ripple phase is preserved down to very low temperatures. The situation is quite analogous to the observations in cholesterol-phosphatidylcholine mixtures.

The limited solubility of the proteins in the crystalline lipid phase leads to the complete exclusion of glycophorin-lipid complexes from the bilayers. There are several indications for this process. In the microfluorescence studies with dye-carrying glycophorin this protein exclusion is clearly seen by an increase in the background fluorescence from the aqueous phase upon lowering the temperature below 10°C. A second indicator is an abrupt decrease in the energy transfer efficiency if the temperature decreases below 10°C. The protein exclusion is a kinetic process which occurs in the time-scale of hours. This shows that extreme care has to be taken in the interpretation of data obtained at low temperatures.

The exclusion of small aggregates below 10°C is most impressively demonstrated in the freeze-fracture electron micrographs by the appearance of the particles (Fig. 5a). These particles are observed at 4°C at protein concentrations greater than 1‰ and their number increases linearly with the protein concentration above this limit. The diameter of the particles is about 80 Å. They could thus well consist of one or two protein molecules incorporated into a lipid micelle. Similar aggregates have been observed by Segrest for the T(is) residue in DPPC bilayers below the phase transition temperature [18].

A characteristic feature of the glycophorin/DMPC system is the large number of lipids interacting with one protein molecule. Obviously this cannot be understood in terms of a pure hydrophobic lipid-protein interaction. According to Marčelja [25] the range of interlipid interaction is of the order of the average lipid distance. Thus the boundary lipid due to a hydrophobic interaction could account for at most 20 lipid molecules. According to our above estimation the carbohydrate-carrying protein headgroup is large enough to explain the above number provided there is a substantial hydrophilic phosphatidylcholine-glycophorin interaction. Such a hydrophilic effect is suggested by the work of Van Zoelen et al. [26], who showed that sialic acid exhibits a perceptible tendency to absorb to phosphatidylcholine-water interfaces. It is expected that the sialic acid-phosphatidylcholine interaction is further amplified by the cooperativity due to the coupling of many sialic acid monomers to macromolecules.

Acknowledgement

Technical assistance by U. Theilen is gratefully acknowledged. This work was supported by the Deutsche Forschungsgemeinschaft under contracts Sa 246 and Ga 233.

References

1 Tomita, M. and Marchesi, V.T. (1975) Proc. Natl. Acad. Sci. U.S.A. 72, 2964–2968
2 Irimura, T., Tsuji, T., Tagami, S., Yamamoto, K. and Osawa, T. (1981) Biochemistry 20, 560–566
3 Yoshima, H., Furthmayr, H. and Kobuta, A. (1980) J. Biol. Chem. 255, 9713–9718
4 Marchesi, V.T. and Furthmayr, H. (1976) Annu. Rev. Biochem. 45, 667–698
5 Grant, C.W.M. and McConnell, H.M. (1974) Proc. Natl. Acad. Sci. U.S.A. 71, 4653–4657
6 Van Zoelen, E.J.J., Van Dijck, P.W.M., De Kruijff, B., Verkleij, A.J. and Van Deenen, L.L.M. (1978) Biochim. Biophys. Acta 514, 9–24
7 Romans, A.Y., Yeagle, P.L., O'Connor, S.E. and Grisham, C.M. (1979) J. Supr. Mol. Struct. 10, 241–251
8 Utsumi, H., Trunggal, B.D. and Stoffel, W. (1980) Biochemistry 19, 2385–2390
9 Dodge, J.T., Mitchell, C. and Hamahan, D.J. (1963) Arch Biochem. Biophys. 100, 119–125
10 Segrest, J.P., Wilkinson, T.M. and Sheng, L. (1979) Biochim. Biophys. Acta 554, 533–537
11 Dohnal, J.C., Potempa, L.A. and Garvin, J.E. (1980) Biochim. Biophys. Acta 621, 255–264
12 MacDonald, R.I. and MacDonald, R.C. (1975) J. Biol. Chem. 250, 9206–9214
13 Cantor, C.R. and Schimmel, P.R. (1980) Biophysical Chemistry, Part II, pp. 439–443, W.H. Freeman, San Francisco
14 Peters, R., Peters, J., Tews, K.H. and Bähr, W. (1974) Biochim. Biophys. Acta 367, 282–294
15 Axelrod, D., Koppel, D.E., Schlessinger, J., Elsan, E. and Webb, W.W. (1976) Biophys. J. 16, 1055–1069
16 Kapitza, H.G. and Sackmann, E. (1980) Biochim. Biophys. Acta 595, 56–64
17 Sackmann, E., Rüppel, D. and Gebhardt, C. (1980) in Springer Series in Chemical Physics (Helfrich, W. and Heppke, G., eds.), Vol. 11, pp. 309–326, Springer Verlag, Berlin, Heidelberg, New York

18 Segrest, J.P. (1977) in Mammalian Cell Membranes (Jamieson, G.A. and Robinson, D.M., eds.), Vol. 3, pp. 1–26, Butterworths, London, Boston
19 Jähnig, F. (1979) J. Chem. Phys. 70, 3279–3290
20 Dewey, T.G. and Hammes, G.G. (1980) Biophys. J. 32, 1023–1036
21 Fung, B.K.K. and Stryer, L. (1978) Biochemistry 17, 5241–5248
22 Kapitza, H.G., Rüppel, D., Galla, H.J. and Sackmann, E. (1982) Biophys. J., submitted
23 De Gennes, P.G. (1979) Scaling Concepts in Polymer Physics, p. 40, Cornell University Press Ithaca and London
24 Sackmann, E., Träuble, H., Galla, H.J. and Overath, P. (1973) Biochemistry 12, 5360–5369
25 Marčelja, S. (1976) Biochim. Biophys. Acta 455, 1–7
26 Van Zoelen, E.J.J., Zwaal, R.F.A., Reuvers, F.A.M., Demel, R.A. and Van Deenen, L.L.M. (1977) Biochim. Biophys. Acta 464, 482–492